Published in final edited form as:

Cell Stem Cell. 2011 August 5; 9(2): 113–118. doi:10.1016/j.stem.2011.07.002.

Direct Reprogramming of Adult Human Fibroblasts to Functional Neurons under Defined Conditions

Rajesh Ambasudhan[1,2], **Maria Talantova**[2], **Ronald Coleman**[1], **Xu Yuan**[1], **Saiyong Zhu**[1,3], **Stuart A. Lipton**[2,*], and **Sheng Ding**[1,3,*]

[1]Department of Chemistry, The Scripps Research Institute, 10550 North Torrey Pines Road, La Jolla, CA 92037, USA

[2]Del E. Webb Center for Neuroscience, Aging, and Stem Cell Research, Sanford-Burnham Medical Research Institute, 10901 North Torrey Pines Road, La Jolla, CA 92037, USA

[3]Gladstone Institute of Cardiovascular Disease, Department of Pharmaceutical Chemistry, University of California, San Francisco, 1650 Owens Street, San Francisco, CA 94158, USA

SUMMARY

Human induced pluripotent stem cells (hiPSCs) have been generated by reprogramming a number of different somatic cell types using a variety of approaches. In addition, direct reprogramming of mature cells from one lineage to another has emerged recently as an alternative strategy for generating cell types of interest. Here we show that a combination of a microRNA (miR-124) and two transcription factors (*MYT1L* and *BRN2*) is sufficient to directly reprogram postnatal and adult human primary dermal fibroblasts (mesoderm) to functional neurons (ectoderm) under precisely defined conditions. These human induced neurons (hiNs) exhibit typical neuronal morphology and marker gene expression, fire action potentials, and produce functional synapses between each other. Our findings have major implications for cell-replacement strategies in neurodegenerative diseases, disease modeling, and neural developmental studies.

The differentiated cell state is often considered stable and resistant to changes in lineage identity. However, challenging this view, differentiated somatic cell types from humans and other organisms have been reprogrammed to the pluripotent state by forced expression of a set of transcription factors (Takahashi et al., 2007), somatic cell nuclear transfer (Campbell et al., 1996; Gurdon et al., 1958), or cell fusion (Cowan et al., 2005; Tada et al., 2001). Additionally, by lineage reprogramming through ectopic expression of selected genes or cell fusion, a few studies have demonstrated that an adult cell type can be directly converted to another adult cell type (Cobaleda et al., 2007; Davis et al., 1987; Feng et al., 2008; Ieda et

*Correspondence: slipton@sanfordburnham.org (S.A.L.), sheng.ding@gladstone.ucsf.edu (S.D.).
X.Y. and R.C. contributed equally to this work.

SUPPLEMENTAL INFORMATION

Supplemental Information for this article includes two figures, two tables, and Supplemental Experimental Procedures (which includes the list of Primers) and can be found with this article online at doi:10.1016/j.stem.2011.07.002.

R.A. conceived the study. R.A., M.T., S.A.L., and S.D. designed experiments. R.A. performed viral infections, generated hiN cells, conducted cellular and molecular characterization, and interpreted the results. R.C. assisted in constructing viral vectors. X.Y. assisted in qPCR analysis and the cell culture. S.Z. assisted in the cell culture. M.T. and S.A.L. designed, performed, and/or analyzed the electrophysiological assays. R.A. and M.T. produced the figures. R.A., S.A.L., and S.D. wrote and/or edited the manuscript.

al., 2010; Zhou et al., 2008; Zhou and Melton, 2008). However, all these studies involve conversion of one cell type to another within the same lineage, a major limitation for many applications. For cell-replacement therapies, the idea of reprogramming across lineages is fascinating because of its potential to rapidly generate a variety of therapeutically important and immunologically matched cell types directly from one's own easily accessible tissues, such as skin or blood. In this context, Vierbuchen et al. (2010) demonstrated that differentiated mouse cells have the capacity for changing lineage by showing direct conversion of dermal fibroblasts to functional "induced neurons" (iNs). Recently, the same group extended these findings to human fetal and postnatal fibroblasts to produce human iN (hiN) cells (Pang et al., 2011). Nonetheless, these hiNs formed functional synapses only when cocultured with mature mouse cortical neurons, which potentially provided additional differentiation factors. Here we show that a combination of a microRNA (miR-124) and two transcription factors (*MYT1L* and *BRN2*) is sufficient to directly reprogram postnatal and adult human primary dermal fibroblasts (mesoderm) to functional neurons (ectoderm) under precisely defined conditions without a requirement for "helper" cells from a different species. These hiNs exhibit typical neuronal morphology and marker gene expression, fire action potentials, and form functional synapses.

Given the known critical roles of specific transcription factors, signaling molecules, and microRNAs in neuronal lineage determination during development or cell fate regulation, we selected 11 transcription factors (Table S1 available online) and a micro-RNA (miR-124) to test for their ability to convert primary postnatal human fibroblasts, BJ or CRL2097, to functional neurons. After confirming the absence of any contaminating neural or neuronal cells in BJ and CRL2097 cell cultures by immunostaining (Figure S1A available online) and RT-PCR (Figure S1B), we transduced them with lentiviruses carrying the 12 factors pooled together (12F pool, with equal representation of each). The subsequent culture conditions are depicted in the schematic diagram in Figure 1A and in the Supplemental Experimental Procedures section. Infected cells were monitored by the presence of red fluorescent protein (RFP) coexpressed with the miRNA vector (pLemiR). Immunocytochemistry for the early neuronal marker βIII-tubulin (Tuj1), performed 18 days after infection, revealed a few Tuj1/RFP double-positive cells that manifested typical neuronal morphology in the 12F-infected cultures (Figure 1B), while no such cells were observed in uninfected or GFP-control cultures (Figures S1A and S1C). These findings suggested that at least some of the factors in the 12F pool had the capacity to convert fibroblasts to human neuronal-like cells.

To test whether any single factor among the 12F pool was sufficient to induce the neuronal phenotype, we transduced BJ cells with the individual factors. Although on day 18 none of these cultures displayed cells with distinctive neuronal morphology, in cultures transduced with miR-124 alone we observed a few Tuj1-positive cells with multiple, small processes that resembled neurites emanating from the soma (Figures S1D and S1E). However, even after continued culturing for over 1 month, these cells did not mature further to produce a characteristic neuronal phenotype (data not shown). Such changes resembled those observed previously when miR-124 was overexpressed in non-neuronal cells (Yu et al., 2008).

Next, we tested two-factor combinations and found that cultures transduced with miR-124 plus *BRN2* (designated mi*B*) or *PAX 6* (mi*P*) exhibited cells that were morphologically

similar to those observed with miR-124 alone, but with >20-fold better efficacy (Figure S1F). Cells infected with miR-124 plus *MYT1L* (mi*M*) showed a distinctive elongated morphology, unique among the combinations that we used (Figure S1G).

Reasoning that some of these four factors might complement one other, we tested three-factor (3F) combinations. Remarkably, within 3 days of transduction with mi*BM*, many RFP-positive BJ cells exhibited small, compact cell bodies with monopolar or bipolar projections and weak βIII-tubulin expression (Figure 1C). A characteristic neuronal morphology, consisting of multiple neuritic extensions and elaborate branching, became progressively obvious when these cells were allowed to mature for an additional 15 days (Figures 1D–1F). The majority of these cells displayed positive immunoreactivity for the mature neuronal markers MAP2 (55%, n = 100) (Figure 1G) and NeuN (46%, n = 100) (Figure 1H). In contrast, we did not observe any neuronal-like cells in cultures transduced with any other 3F combinations (data not shown) or in control cultures where miR-124 was replaced with scrambled, nonspecific small RNAs (Figure 1I). Also, the addition of more factors to mi*BM* did not substantially improve the process. CRL2097 fibroblasts produced similar results to BJ cells (data not shown).

An EdU incorporation assay suggested that fibroblasts destined to become hiN cells were most likely postmitotic within 24 hr of transgene induction, and thus it is likely that hiN conversion occurred in the absence of a mitotic progenitor cell stage (Figures S1H–S1P). By dividing the number of Tuj1-positive hiN cells on day 18 by the total number of cells in the starting fibroblast population, we estimated an efficiency of 4%–8% for hiN generation from BJ or CRL2097 human fibroblast cells (Figure S1Q). Furthermore, and importantly, using a doxycycline or cumate-inducible system, we found that expression of mi*BM* for 7 days was sufficient to produce hiN cells at a frequency comparable to that of our earlier experiments (Figure 1A and Figures S2A–S2G).

To functionally characterize hiN cells derived with mi*BM*, we examined their electrophysiological properties on day 25 when the vast majority of cells displayed synapsin immunoreactivity (Figures 2A and 2B), a marker associated with functional maturation of neuronal synapses. During whole-cell recording in voltage-clamp mode, the majority of hiN cells (60%, n = 10) exhibited rapidly inactivating inward current with a rise time of 2–3 ms, followed by outward currents, most likely corresponding to opening of voltage-dependent Na^+ and K^+ channels, respectively (Figure 2C). The inward current was inhibited by the sodium channel blocker tetrodotoxin (Figure 2D). In current-clamp mode, the resting membrane potential averaged about −45 mV, and with increasing time in culture the majority of cells (81%, n = 29) fired action potentials with amplitudes of ~110 mV in response to injection of 10 to 20 pA currents (Figure 2E). Some hiN cells (~15%) exhibited spontaneous action potentials (Figure 2F, left panel), and others (~20%), repetitive trains of evoked action potentials (Figure 2F, right panel). We also monitored additional electrophysiological parameters, including membrane capacitance, access resistance, and total membrane resistance (Table S2A); these values are consistent with the notion that the hiN cells were maturing neurons.

We next examined whether the hiN cells manifested functional neurotransmitter properties by testing for specific markers and corresponding ligand-gated currents. Immunostaining revealed that about 8% of hiN cells (n = 50) were positive for the inhibitory neurotransmitter GABA (Figures 2G and 2H), and 12% manifested punctuate staining for VGAT (data not shown), a protein involved in vesicular transport of GABA. Importantly, hiN cells responded to exogenous application of GABA (60%, n = 5), producing whole-cell currents (Figure 2I).

Furthermore, we recorded slowly decaying NMDA-evoked current in 67% (n = 6) of hiN cells (Figure 2J). Moreover, a high percentage of hiN cells displayed presynaptic properties of excitatory glutamatergic neurons, as indicated by positive VGLUT1 staining (44%, n = 50) (Figures 2K and 2L), a marker for the vesicular glutamate transporter. While we observed rare hiN cells of dopaminergic-like phenotype, as evidenced by tyrosine hydroxylase staining (Figures 2M and 2N), none stained for peripherin, choline acetyltransferase, or serotonin (data not shown).

By day 30 postinfection, patch-clamp recordings revealed miniature excitatory postsynaptic currents (mEPSCs), indicative of functional synapses, in 25% (n = 8) of hiN cells (Figure 2O, top panel). These currents were sensitive to NBQX, an AMPA-type glutamate receptor antagonist, but not bicuculline, a competitive inhibitor of $GABA_A$ receptors (Figure 2O, bottom panel), thus further confirming their excitatory nature. These results further substantiate the functional neurotransmitter properties of hiN cells derived from postnatal human fibroblasts, and collectively provide strong evidence that the cells had become functional neurons that generated synaptic connections.

Finally, to examine whether adult human fibroblasts could generate hiN cells, we tested dermal fibroblasts derived from abdominal skin of a 55-year-old Caucasian female (aHDF-1) and breast skin of a 41-year-old Caucasian female (aHDF-2). After confirming that these cells were free of contaminating neural or spinal progenitor cells, neurons, or epidermal keratinocytes (Figures S1A and S1B), we transduced them with viruses carrying the mi*BM* transgenes. Similar to our observations on postnatal fibroblasts, these adult human fibroblasts were converted to hiN cells with an efficiency of 1.5%–2.9% (aHDF-1) or 9.5%–11.2% (aHDF-2) (Figure S1Q), and displayed characteristic mature neuronal morphology and marker gene expression (Figures 2P–2R).

When tested on day 25 postinfection, hiN cells derived from adult fibroblasts also exhibited rapidly inactivating Na^+ currents (47%, n = 17) and fired action potentials (12%, n = 25) (Figures 2S and 2T). The mean action potential amplitude was 73.4 ± 18.3 mV (mean ± SEM). Values for resting membrane potential, membrane capacitance, access resistance, and total membrane resistance (Table S2B) were comparable to those of BJ or CRL2097-derived hiN cells, except that the greater membrane resistance probably reflected their more immature nature. Moreover, many of these cells exhibited VGLUT1 immunoreactivity (28%, n = 50) (Figure 2U) and NMDA-evoked responses (60%, n = 5) (Figure 2V), thus displaying excitatory neuronal properties. Additionally, when plated at high density, but not low density, aHDF-hiN cells displayed excitatory synaptic currents (43%, n = 7) (Figure 2W), reflecting functional contacts with neighboring hiNs.

Therefore, we have demonstrated here that a combination of miR-124, *BRN2*, and *MYT1L* can induce rapid reprogramming of postnatal and adult human fibroblasts into functional neurons. While other combinations of transcription factors have recently been reported to produce neuronal-like cells from human fibroblasts (Pang et al., 2011) and dopaminergic neurons (Pfisterer et al., 2011; Caiazzo et al., 2011), an important development with our combined microRNA/transcription factor approach is that we have been able to produce neurons with mature functional synapses between adult fibroblast-derived hiNs in the absence of other cell types.

Along these lines, in our study reprogramming was ineffective for combinations of factors lacking miR-124. miR-124, the most abundant microRNA in the mammalian CNS (Lagos-Quintana et al., 2002), is markedly upregulated in differentiating and mature neurons (Deo et al., 2006), where it modulates the activity of major antineuronal differentiation factors, including REST/SCP1 (Conaco et al., 2006; Visvanathan et al., 2007), PTBP1 (Makeyev et al., 2007), SOX9 (Cheng et al., 2009), and npBAF complex (Yoo et al., 2009). Moreover, miR-124 targets more than 1000 genes, many of which are downregulated during neuronal differentiation (Lewis et al., 2005). Interestingly, introduction of miR-124 to HeLa cells could transform their gene expression pattern to resemble that of brain tissue (Lim et al., 2005). However, overexpression of miR-124 by itself seems to be insufficient to induce neurogenesis, but rather ensured that nonneuronal genes were posttranscriptionally inhibited in neurons (Cao et al., 2007). In line with these observations, in our experiments miR-124 only effected neuronal reprogramming in the presence of other key factors. The reprogramming platform described here provides rapid conversion of adult cell types directly into neurons, as opposed to more time-consuming and labor-intensive iPSC or ESC-based methods. Our findings also provide a technology that can use patient-specific cells for the rapid production of models of various human neurodegenerative “diseases in a dish,” including diseases that are only manifest later in life.

Supplementary Material

Refer to Web version on PubMed Central for supplementary material.

ACKNOWLEDGMENTS

We would like to thank Marius Wernig (Stanford University) for the generous gift of pBrn2-TetO-FUW and pMyt1l-TetO-FUW plasmids. We thank all members of the Ding lab for helpful discussions, and Wenlin Li and Jem Efe for critical reading of the manuscript. M.T. and S.A.L. were supported in part by NIH grants P01 HD29587, P01 ES016738, P30 NS057096, and R01 EY05477, and by the California Institute for Regenerative Medicine. S.D. was supported by funding from NICHD, NHLBI, NEI, and NIMH/NIH, California Institute for Regenerative Medicine, Prostate Cancer Foundation, Fate Therapeutics, and the Gladstone Institutes.

REFERENCES

Caiazzo M, Dell’anno MT, Dvoretskova E, Lazarevic D, Taverna S, Leo D, Sotnikova TD, Menegon A, Roncaglia P, Colciago G, et al. Direct generation of functional dopaminergic neurons from mouse and human fibroblasts. Nature. 2011

Campbell KH, McWhir J, Ritchie WA, Wilmut I. Sheep cloned by nuclear transfer from a cultured cell line. Nature. 1996; 380:64–66. [PubMed: 8598906]

Cao X, Pfaff SL, Gage FH. A functional study of miR-124 in the developing neural tube. Genes Dev. 2007; 21:531–536. [PubMed: 17344415]

Cheng LC, Pastrana E, Tavazoie M, Doetsch F. miR-124 regulates adult neurogenesis in the subventricular zone stem cell niche. Nat. Neurosci. 2009; 12:399–408. [PubMed: 19287386]

Cobaleda C, Jochum W, Busslinger M. Conversion of mature B cells into T cells by dedifferentiation to uncommitted progenitors. Nature. 2007; 449:473–477. [PubMed: 17851532]

Conaco C, Otto S, Han JJ, Mandel G. Reciprocal actions of REST and a microRNA promote neuronal identity. Proc. Natl. Acad. Sci. USA. 2006; 103:2422–2427. [PubMed: 16461918]

Cowan CA, Atienza J, Melton DA, Eggan K. Nuclear reprogramming of somatic cells after fusion with human embryonic stem cells. Science. 2005; 309:1369–1373. [PubMed: 16123299]

Davis RL, Weintraub H, Lassar AB. Expression of a single transfected cDNA converts fibroblasts to myoblasts. Cell. 1987; 51:987–1000. [PubMed: 3690668]

Deo M, Yu JY, Chung KH, Tippens M, Turner DL. Detection of mammalian microRNA expression by in situ hybridization with RNA oligonucleotides. Dev. Dyn. 2006; 235:2538–2548. [PubMed: 16736490]

Feng R, Desbordes SC, Xie H, Tillo ES, Pixley F, Stanley ER, Graf T. PU.1 and C/EBPalpha/beta convert fibroblasts into macrophage- like cells. Proc. Natl. Acad. Sci. USA. 2008; 105:6057–6062. [PubMed: 18424555]

Gurdon JB, Elsdale TR, Fischberg M. Sexually mature individuals of Xenopus laevis from the transplantation of single somatic nuclei. Nature. 1958; 182:64–65. [PubMed: 13566187]

Ieda M, Fu JD, Delgado-Olguin P, Vedantham V, Hayashi Y, Bruneau BG, Srivastava D. Direct reprogramming of fibroblasts into functional cardiomyocytes by defined factors. Cell. 2010; 142:375–386. [PubMed: 20691899]

Lagos-Quintana M, Rauhut R, Yalcin A, Meyer J, Lendeckel W, Tuschl T. Identification of tissue-specific microRNAs from mouse. Curr. Biol. 2002; 12:735–739. [PubMed: 12007417]

Lewis BP, Burge CB, Bartel DP. Conserved seed pairing, often flanked by adenosines, indicates that thousands of human genes are microRNA targets. Cell. 2005; 120:15–20. [PubMed: 15652477]

Lim LP, Lau NC, Garrett-Engele P, Grimson A, Schelter JM, Castle J, Bartel DP, Linsley PS, Johnson JM. Microarray analysis shows that some microRNAs downregulate large numbers of target mRNAs. Nature. 2005; 433:769–773. [PubMed: 15685193]

Makeyev EV, Zhang J, Carrasco MA, Maniatis T. The MicroRNA miR-124 promotes neuronal differentiation by triggering brain-specific alternative pre-mRNA splicing. Mol. Cell. 2007; 27:435–448. [PubMed: 17679093]

Pang ZP, Yang N, Vierbuchen T, Ostermeier A, Fuentes DR, Yang TQ, Citri A, Sebastiano V, Marro S, Südhof TC, Wernig M. Induction of human neuronal cells by defined transcription factors. Nature. 2011

Pfisterer U, Kirkeby A, Torper O, Wood J, Nelander J, Dufour A, Björklund A, Lindvall O, Jakobsson J, Parmar M. Direct conversion of human fibroblasts to dopaminergic neurons. Proc. Natl. Acad. Sci. USA. 2011; 108:10343–10348. [PubMed: 21646515]

Tada M, Takahama Y, Abe K, Nakatsuji N, Tada T. Nuclear reprogramming of somatic cells by in vitro hybridization with ES cells. Curr. Biol. 2001; 11:1553–1558. [PubMed: 11591326]

Takahashi K, Tanabe K, Ohnuki M, Narita M, Ichisaka T, Tomoda K, Yamanaka S. Induction of pluripotent stem cells from adult human fibroblasts by defined factors. Cell. 2007; 131:861–872. [PubMed: 18035408]

Vierbuchen T, Ostermeier A, Pang ZP, Kokubu Y, Südhof TC, Wernig M. Direct conversion of fibroblasts to functional neurons by defined factors. Nature. 2010; 463:1035–1041. [PubMed: 20107439]

Visvanathan J, Lee S, Lee B, Lee JW, Lee SK. The microRNA miR-124 antagonizes the anti-neural REST/SCP1 pathway during embryonic CNS development. Genes Dev. 2007; 21:744–749. [PubMed: 17403776]

Yoo AS, Staahl BT, Chen L, Crabtree GR. MicroRNA-mediated switching of chromatin-remodelling complexes in neural development. Nature. 2009; 460:642–646. [PubMed: 19561591]

Yu JY, Chung KH, Deo M, Thompson RC, Turner DL. MicroRNA miR-124 regulates neurite outgrowth during neuronal differentiation. Exp. Cell Res. 2008; 314:2618–2633. [PubMed: 18619591]

Zhou Q, Melton DA. Extreme makeover: converting one cell into another. Cell Stem Cell. 2008; 3:382–388. [PubMed: 18940730]

Zhou Q, Brown J, Kanarek A, Rajagopal J, Melton DA. in vivo reprogramming of adult pancreatic exocrine cells to beta-cells. Nature. 2008; 455:627–632. [PubMed: 18754011]

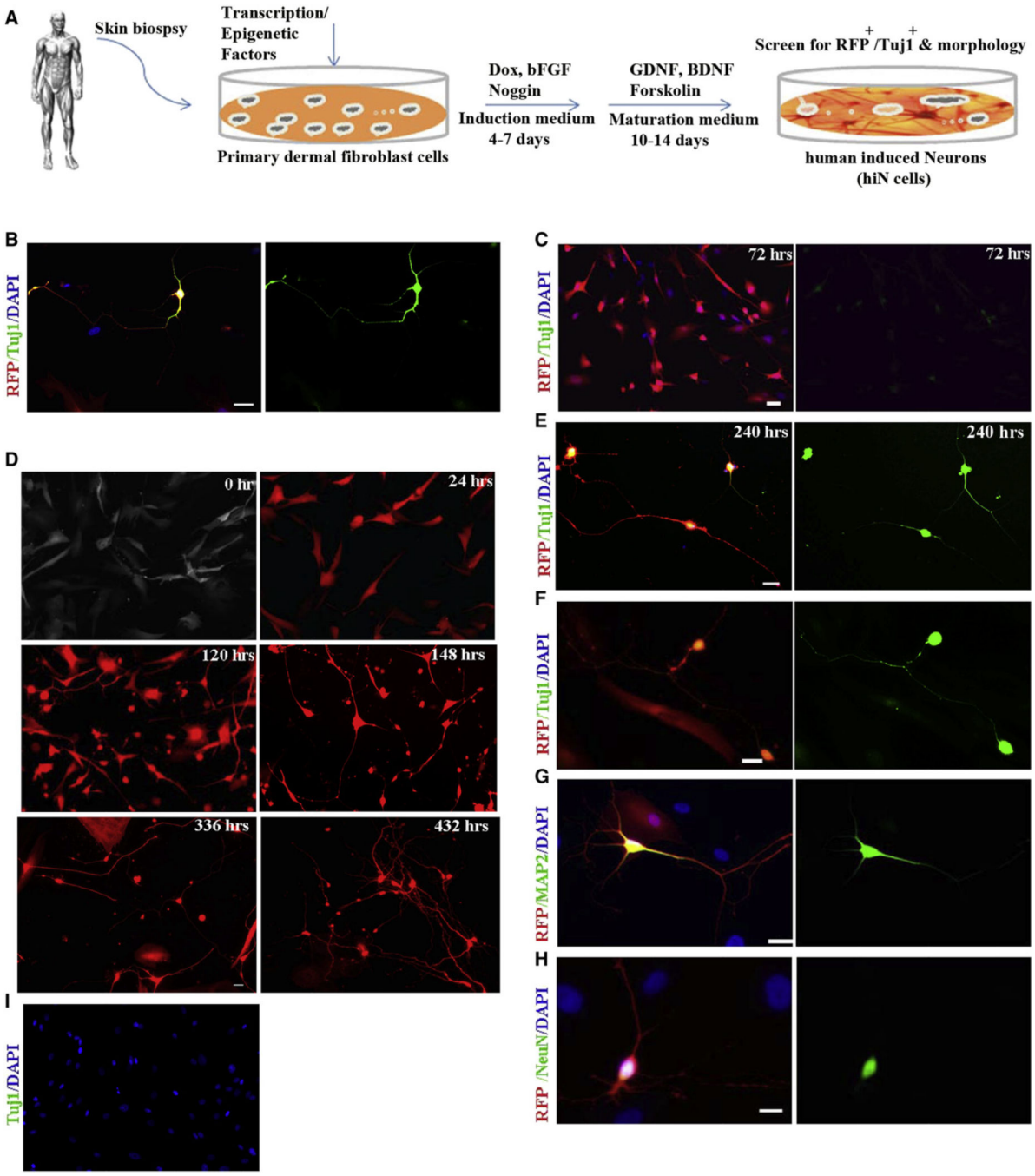

Figure 1. Conversion of Postnatal Human Dermal Fibroblasts to hiN Cells using Defined Factors under Defined Conditions

(A) Schematic showing the experimental protocol.

(B) Tuj1-stained hiN cells 18 days after infection of BJ cells with the 12F pool.

(C) Within 3 days of infection, 3F (mi*BM*)-transduced fibroblasts exhibited notable morphological changes and weak immunoreactivity with Tuj1 antibody.

(D) Time-lapse live images of RFP^+ BJ cells infected with mi*BM* showed gradual changes leading to neuronal-like morphology.

(E) 3F-infected BJ cells were $Tuj1^+$ and exhibited characteristic neuronal morphology when stained 240 hr (10 days) after infection.
(F–H) By day 18, hiN cells expressed, in addition to Tuj1 (F), mature neuronal markers, including MAP2 (G) and NeuN (H).
(I) Control cultures infected with *BM* transgenes along with nonspecific scrambled RNA did not generate hiN cells or show immunoreactivity to Tuj1 antibody.
Red: RFP; green: Tuj1 (B, C, E, F, and I), MAP2 (G), or NeuN (H); blue: DAPI. Scale: 20 μm. See also Figure S1 and Table S1.

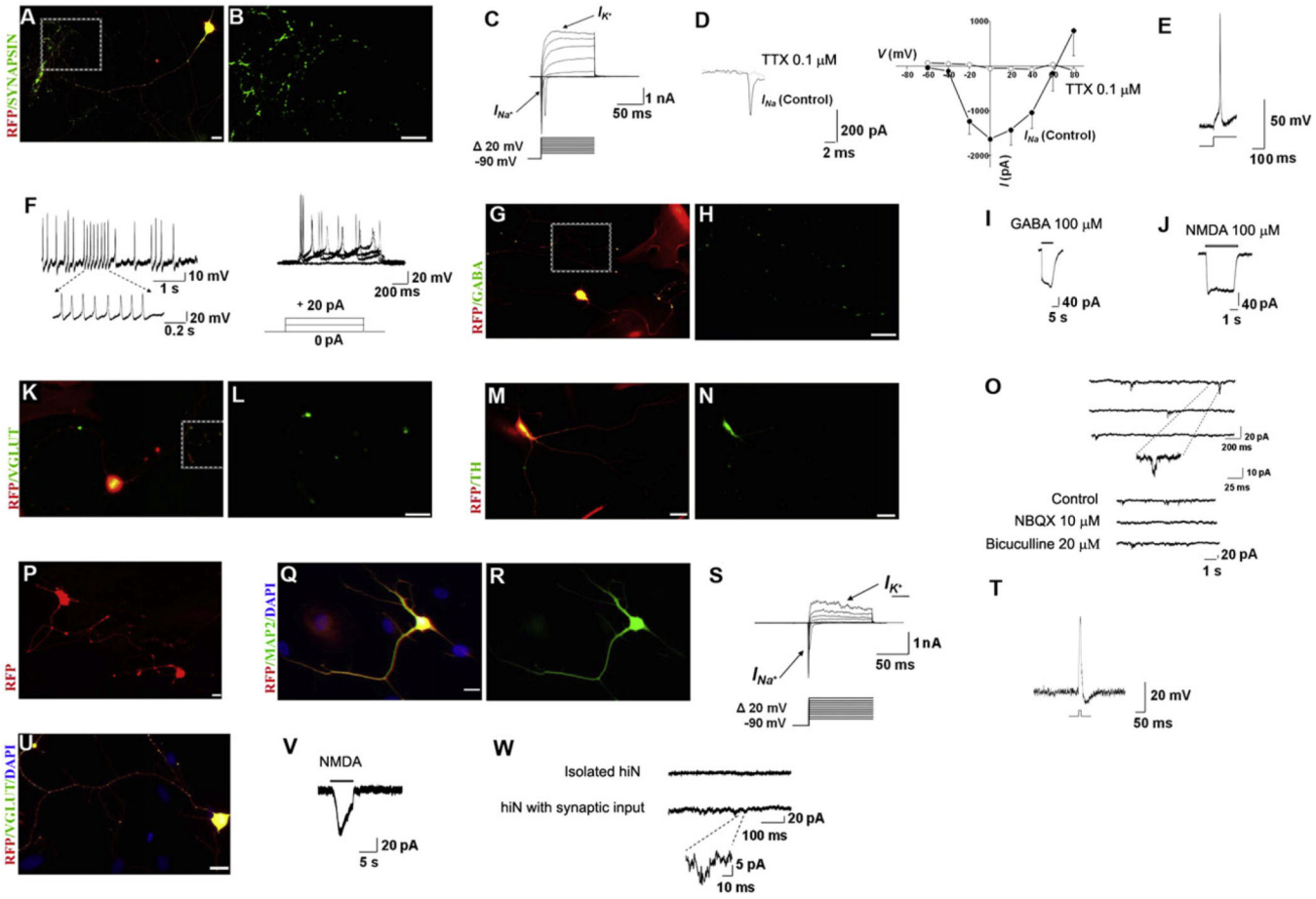

Figure 2. hiN Cells from Postnatal and Adult Human Fibroblasts Show Functional Maturation and Synaptic Properties

(A and B) hiN cells, assessed 25 days postinfection, stained positively for synapsin-1.

(C) Representative traces of whole-cell currents recorded in voltage-clamp mode. Cells were hyperpolarized to −90 mV for 300 ms before depolarizing pulses were applied to elicit Na^+ and K^+ currents.

(D) The inward currents could be blocked by Na^+ channel blocker tetrodotoxin (TTX). CsCl was present in the patch electrode-filling solution to suppress K^+ currents. Representative current traces recorded in the presence of TTX are shown at left, and the current-voltage (I/V) relationship, at right (mean + SEM, n = 13).

(E and F) Traces of evoked (E) and spontaneous (F, left panel) action potentials recorded in current-clamp mode on day 25. In other hiN cells, repetitive trains of evoked action potentials were observed after transgene inactivation (F, right panel).

(G and H) hiN cells expressing GABA.

(I) GABA-evoked current from hiN cell at a holding potential of −80 mV.

(J–L) Other hiN cells responded to application of exogenous NMDA in the nominal absence of extracellular Mg^{2+} (J) and expressed glutamate transporter VGLUT (K and L).

(M and N) hiN cell staining for tyrosine hydroxylase (TH) on day 25.

(O) Top panel: Representative traces of mEPSCs recorded at a holding potential of −80 mV in hiN cells on day 30 in culture, indicating functional synapse formation. The insert

demonstrates the rapid kinetics of these synaptic currents. Bottom panel: Spontaneous synaptic currents were reversibly inhibited by addition of 10 μM NBQX (to block excitatory AMPA-type glutamate receptors), but not by 20 μM bicuculline (to block inhibitory GABA receptors).

(P) Representative image of live aHDF-converted hiN cells on day 18 postinfection exhibiting typical neuronal morphology and RFP fluorescence.

(Q and R) aHDF-converted hiN cells displayed mature neuronal marker MAP2 when fixed and immunostained 18 days after 3F (mi*BM*) infection.

(S) Representative traces of whole-cell currents in voltage-clamp mode from aHDF-converted hiN cells 25 days postinfection. Cells were hyperpolarized to −90 mV for 300 ms before depolarizing pulses were applied to elicit Na^+ and K^+ currents.

(T) Representative action potential recorded in current-clamp mode.

(U) Day 25 aHDF-converted hiN cell displaying immunoreactivity for VGLUT antibody.

(V) Patch-clamp recording showing response of day 25 aHDF-converted hiN cell to application of exogenous NMDA in the nominal absence of Mg^{2+} in the bath solution.

(W) Spontaneous synaptic currents from an aHDF hiN cell plated at high density (lower trace), reflecting mEPSCs given the composition of the intracellular and bath solutions used in the recording (see Experimental Procedures). The magnified trace shows the rapid kinetics of an mEPSC. When plated at lower density to isolate the cells, aHDF hiNs were synaptically silent (upper trace).

Red: RFP; green: synapsin (B), GABA (H), VGLUT (L), TH (N), MAP2 (R), and VGLUT (U); blue: DAPI stained nuclei (Q and U). Boxed areas in the left-hand panels (A, G, and K) are shown at higher magnification in the adjacent right-hand panels (B, H, and L). Large red cells in (G), (K), (M), and (Q) are infected fibroblasts expressing RFP that have not undergone conversion to hiN cells. (A), (G), (K), (M), (Q), and (U) are merged images. Scale bars: 20 μm. See also Figure S2 and Table S2.